



Available online at <http://scik.org>

J. Math. Comput. Sci. 11 (2021), No. 2, 2092-2111

<https://doi.org/10.28919/jmcs/5403>

ISSN: 1927-5307

ROTATING MHD CONVECTIVE HEAT AND MASS TRANSFER FLOW WITH RAMPED TEMPERATURE AND CONCENTRATION UNDER THE EFFECTS OF RADIATION, CHEMICAL REACTION AND HALL CURRENT

P. J. PARASHAR*, N. AHMED

Department of Mathematics, Gauhati University, Guwahati-781014, India

Abstract: An analytic solution to a problem of MHD heat and mass transfer flow of an incompressible, viscous, electrically conducting, partially ionized, heat absorbing and chemically reacting fluid in the presence of thermal radiation and Hall current with ramped temperature and concentration has been presented. In the entire investigation, only the externally applied magnetic field is taken into consideration and the induced magnetic field is neglected. Laplace Transform technique in closed form is adopted to solve the governing equations of the motion describing the velocity, temperature and concentration profiles. The effects of the relevant physical parameters on these fields and also on skin friction, Nusselt number and Sherwood number are displayed and discussed through graphs.

Keywords: Hall current; Coriolis force; thermal radiation; chemical reaction; ramped concentration.

2010 AMS Subject Classification: 76W05.

1. INTRODUCTION

MHD fluid flow model has been a field of great attraction among researchers over the past decades due to its wide range of applications in Astrophysics, Geophysics, Aerodynamics, Plasma Physics etc. Later, many researchers started considering the Hall effect in the MHD convective flow

*Corresponding author

E-mail address: parasharpranabjyoti@gmail.com

Received January 9, 2021

problems. Generally, Hall effect is not considered in the Ohm's law. But a strong applied magnetic field induces a considerable current in the direction perpendicular to both the fluid velocity and the applied magnetic field. So a secondary flow is induced in such cases which cannot be neglected. This was first reported by Cowling [1]. Later Pop [2] analyzed the effect of Hall currents on hydromagnetic flow near an accelerated plate. Its importance in the Hartmann channel flows was discussed by Cramer and Pai [3]. Due to the practical applications of Hall effects in MHD generators and Hall accelerators, researchers are continuously being attracted towards the investigation of Hall effects on MHD convective flows. Takhar et al. [4], Malique and Sattar [5] are some names in this regard. As rotation (Coriolis force) also induces secondary flow, authors including Ahmed and Sarma [6], Ghosh et al. [7], Seth et al. [8], Seth et al. [9] have also considered the rotation effect along with the Hall effect to study the combined and comparative effects of both the factors on MHD fluid flows.

Generally, the study of MHD fluid flow models also includes the heat and mass transfer characteristics along with the flow characteristics. In case of heat transfer, apart from convective heat transfer, heat transfer by radiation is also a matter of great interest among researchers. Radiation is encountered in various industrial and physical processes. Processes such as cooling of nuclear reactors, fossil fuel combustion, astrophysical flows, heating and cooling of chambers etc. and in general all the processes concerning with high temperature involve the phenomenon of radiation. Ali et al. [10], Mansour [11], Makinde [12], Mbeledogu [13], Ahmed [14], Ahmed [15], Choudhury and Ahmed [16] are some of the authors among many who have included heat transfer by radiation in their work. The phenomenon of mass transfer by free convection can be observed in processes such as evaporation of alcohol and the principles of mass transfer are applied in various fields of geophysics, astrophysics, metallurgy, home humidifiers, MHD pumps etc. Again rate of chemical reaction and species concentration affect each other. Consequently, chemical reaction affects the mass transfer process as well. Jena et al. [17] studied the chemical reaction effect on MHD flow of viscoelastic fluid. Gurram et al. [18] studied the chemical reaction effect and radiation effect on MHD Casson fluid flow.

This paper generalizes the work of Seth et al. [9] to study the effects of radiation and chemical reaction which were not included in their study. Further in their work, after the start of the motion concentration at the plate was assumed to remain constant. But in the present work, both the temperature and concentration at the plate are set to be ramped. As chemical reaction can affect the species concentration, a ramped concentration is more justified than a throughout constant concentration at the plate.

2. MATHEMATICAL ANALYSIS

We consider the natural convective motion of an incompressible, viscous, electrically conducting, partially ionized, heat absorbing, radiating and chemically reacting fluid past a semi-infinite plate through a uniformly porous medium. A rectangular Cartesian co-ordinate system is introduced so that the two mutually perpendicular edges of the rectangular plate become the X' and Z' axes, with the one in the vertically upward direction being the X' axis, and perpendicular to the plate and directed towards the fluid region is chosen to be the Y' axis.

The fluid as well as the plate is assumed to be rotating about the Y' axis with constant angular speed ω . It is assumed that an external strong magnetic field \vec{B} of intensity B_0 acts along the positive Y' direction. At time $t' = 0$, the system is at rest and the temperature and the concentration at the plate are same with the free stream fluid temperature T'_∞ and the free stream fluid concentration C'_∞ respectively. At time $t' > 0$, the plate starts moving in its own plane with initial velocity U_0 in the vertically upward direction. Also, the plate temperature and concentration at the plate start varying till time $t' = t_0$ and after time $t' > t_0$, the temperature and concentration at the plate become unchanged. Thus attained constant temperature and concentration are assumed to be T'_w and C'_w respectively.

In the present investigation, induced magnetic field is neglected as the magnetic Reynolds number is assumed to be very small. But, as the intensity of the applied magnetic field \vec{B} is assumed to

be very strong, the Lorentz force arising due to the interactions of the partially ionized moving fluid and the magnetic field \vec{B} induces a considerable current in the transverse direction known as the Hall current. Considering the Hall current, the electric current density vector $\vec{J} = (J_{x'}, J_{y'}, J_{z'})$ for the problem is given by,

$$\left. \begin{aligned} J_{x'} &= [\alpha_1 (E_{x'} - B_0 W') + \beta_1 (E_{z'} + B_0 U')] \sigma \\ J_{y'} &= 0 \text{ (the plate considered is electrically non-conducting)} \\ J_{z'} &= [\alpha_1 (E_{z'} + B_0 U') - \beta_1 (E_{x'} - B_0 W')] \sigma \end{aligned} \right\} \quad (1)$$

$$\text{where, } \alpha_1 = \frac{1}{1 + (\beta_e)^2}, \beta_1 = \frac{\beta_e}{1 + (\beta_e)^2}$$

With \vec{J} given by (1), together with the infinite plate assumption, the momentum conservation equations for the problem are given as:

$$\rho \left(\frac{\partial U'}{\partial t'} + 2\omega W' \right) = \mu \frac{\partial^2 U'}{\partial y'^2} - \frac{\partial p}{\partial x'} - J_{z'} B_0 - \frac{\mu U'}{Kp^*} - \rho g \quad (2)$$

$$\rho \left(\frac{\partial W'}{\partial t'} - 2\omega U' \right) = \mu \frac{\partial^2 W'}{\partial y'^2} - \frac{\partial p}{\partial y'} + J_{x'} B_0 - \frac{\mu W'}{Kp^*} \quad (3)$$

Far away from the plate, in the free stream, it is assumed that $U' = W' = 0, \rho = \rho_\infty$. With this assumption, Equations (2) and (3) in the free stream take the form:

$$\frac{\partial p}{\partial x'} = (-\alpha_1 E_{z'} + \beta_1 E_{x'}) B_0 \sigma - \rho_\infty g \quad (4)$$

$$\frac{\partial p}{\partial y'} = (\beta_1 E_{z'} + \alpha_1 E_{x'}) B_0 \sigma \quad (5)$$

It is recalled the equation of state based on the classical Bousinnesq approximation:

$$\rho_\infty = \rho + \rho\beta(T' - T'_\infty) + \rho\beta^*(C' - C'_\infty) \quad (6)$$

On implementation of Equations (4), (5) and (6), Equations (2) and (3) become:

$$\frac{\partial U'}{\partial t'} + 2\omega W' = \nu \frac{\partial^2 U'}{\partial y'^2} - \frac{B_0^2 \sigma}{\rho} (\beta_1 W' + \alpha_1 U') - \frac{\nu U'}{Kp^*} + \beta g (T' - T'_\infty) + \beta^* g (C' - C'_\infty) \quad (7)$$

$$\frac{\partial W'}{\partial t'} - 2\omega U' = \nu \frac{\partial^2 W'}{\partial y'^2} + \frac{B_0^2 \sigma}{\rho} (\beta_1 U' - \alpha_1 W') - \frac{\nu W'}{Kp^*} \quad (8)$$

With the assumption that viscous and Ohmic dissipations of energy are negligible, the energy equation for the heat absorbing and radiating moving fluid is given by:

$$\frac{\partial T'}{\partial t'} = \frac{\kappa}{\rho C_p} \frac{\partial^2 T'}{\partial y'^2} - \frac{1}{\rho C_p} \frac{\partial q_r}{\partial y'} - \frac{Q'}{\rho C_p} (T' - T'_\infty) \quad (9)$$

The radiation heat flux is considered only along the direction of normal to the plate. Approximation on the basis of Rossland model gives,

$$q_r = -\frac{4\sigma^*}{3a^*} \frac{\partial T'^4}{\partial y'} \quad (10)$$

Assuming the quantity $(T' - T'_\infty)$ to be very small, the Taylor series expansion of T'^4 about $(T' - T'_\infty)$ is approximated as,

$$T'^4 = 4T_\infty'^3 T' - 3T_\infty'^3 \quad (11)$$

Due to (10) and (11), Equation (9) takes the form:

$$\rho C_p \frac{\partial T'}{\partial t'} = \kappa \frac{\partial^2 T'}{\partial y'^2} + \frac{16\sigma^* T_\infty'^3}{3a^*} \frac{\partial^2 T'}{\partial y'^2} - Q' (T' - T'_\infty) \quad (12)$$

The species continuity equation for the chemically reacting moving fluid is found as:

$$\frac{\partial C'}{\partial t'} = D_M \frac{\partial^2 C'}{\partial y'^2} - K_1 (C' - C'_\infty) \quad (13)$$

The initial and boundary conditions of the flow model are assumed to be:

$$\left. \begin{aligned}
 t' \leq 0, y' = 0: U' = 0, W' = 0, T' = T'_\infty, C' = C'_\infty \\
 t' > 0, y' = 0: U' = U_0, W' = 0 \\
 T' = T'_\infty + (T'_w - T'_\infty) \frac{t'}{t_0}, C' = C'_\infty + (C'_w - C'_\infty) \frac{t'}{t_0} \text{ for } 0 < t' < t_0 \\
 T' = T'_w, C' = C'_w \text{ for } t' > t_0 \\
 t' > 0, y' \rightarrow \infty: U' \rightarrow 0, W' \rightarrow 0, T' \rightarrow T'_\infty, C' \rightarrow C'_\infty
 \end{aligned} \right\} \quad (14)$$

Following non-dimensional quantities are defined:

$$\left. \begin{aligned}
 U = \frac{U'}{U_0}, W = \frac{W'}{U_0}, t = \frac{t'}{t_0}, y = \frac{y'}{U_0 t_0}, \theta = \frac{T' - T'_\infty}{T'_w - T'_\infty} \\
 \phi = \frac{C' - C'_\infty}{C'_w - C'_\infty}, Gr = \frac{g \beta v (T'_w - T'_\infty)}{U_0^3}, Gm = \frac{g \beta^* v (C'_w - C'_\infty)}{U_0^3} \\
 Er^2 = \frac{\omega v}{U_0^2}, M^2 = \frac{B_0^2 v \sigma}{\rho U_0^2}, Kp = \frac{Kp^* U_0^2}{v^2}, Ra = \frac{U_0^2 t_0}{v}, N = \frac{\kappa a^*}{4 \sigma^* T_\infty^{*3}}, \\
 Pr = \frac{\mu C_p}{\kappa}, K = \frac{K_1 v}{U_0^2}, Sc = \frac{v}{D_M}, Q = \frac{Q' v}{\rho C_p U_0^2}
 \end{aligned} \right\} \quad (15)$$

Due to (15), Equations (7), (8), (12) and (13) take the non-dimensional form as:

$$\frac{\partial U}{\partial t} + 2WEr^2 Ra = \frac{1}{Ra} \frac{\partial^2 U}{\partial y^2} - M^2 Ra (\beta_1 W + \alpha_1 U) - \frac{RaU}{Kp} + Ra(Gr\theta + Gm\phi) \quad (16)$$

$$\frac{\partial W}{\partial t} - 2UEr^2 Ra = \frac{1}{Ra} \frac{\partial^2 W}{\partial y^2} + M^2 Ra (\beta_1 U - \alpha_1 W) - \frac{RaW}{Kp} \quad (17)$$

$$\frac{\partial \theta}{\partial t} = \frac{1}{Pr Ra} \left(1 + \frac{4}{3N} \right) \frac{\partial^2 \theta}{\partial y^2} - Q Ra \theta \quad (18)$$

$$\frac{\partial \phi}{\partial t} = \frac{1}{Sc Ra} \frac{\partial^2 \phi}{\partial y^2} - K Ra \phi \quad (19)$$

With the introduction of the variable $q = U + iW$, Equations (16) and (17) are combined to transform into the Equation (20).

$$\frac{\partial q}{\partial t} = \frac{1}{Ra} \frac{\partial^2 q}{\partial y^2} + Ra(Gr\theta + Gm\phi) - \lambda q \quad (20)$$

The initial and boundary conditions (14) are also made dimensionless with the help of (15) as:

$$\left. \begin{aligned} t \leq 0, y = 0: q = 0, \theta = 0, \phi = 0 \\ t > 0, y = 0: q = 1 \\ \theta = t, \phi = t \text{ for } 0 < t \leq 1 \\ \theta = 1, \phi = 1 \text{ for } t > 1 \\ t > 0, y \rightarrow \infty: q \rightarrow 0, \theta \rightarrow 0, \phi \rightarrow 0 \end{aligned} \right\} \quad (21)$$

3. METHOD OF SOLUTION

Governing equations (20), (18) and (19) are subjected to Laplace transformations. This transforms the partial differential equations into ordinary differential equations given by (22), (23) and (24) respectively:

$$\frac{d^2 \bar{q}}{dy^2} - Ra(s + \lambda) \bar{q} = -Ra^2 (\text{Gr} \bar{\theta} + \text{Gm} \bar{\phi}) \quad (22)$$

$$\frac{d^2 \bar{\theta}}{dy^2} - \left(\frac{s + \lambda_3}{\lambda_2} \right) \bar{\theta} = 0 \quad (23)$$

$$\frac{d^2 \bar{\phi}}{dy^2} - \left(\frac{s + \lambda_5}{\lambda_4} \right) \bar{\phi} = 0 \quad (24)$$

It is to be noted that Laplace transform of any function $f(y, t)$ has been denoted by $\bar{f}(y, s)$.

The Laplace transformations of the initial and boundary conditions (21) are obtained as follow:

$$\left. \begin{aligned} y = 0: \bar{q} = \frac{1}{s}, \bar{\theta} = \bar{\phi} = \frac{1}{s^2} (1 - e^{-s}) \\ y \rightarrow \infty: \bar{q} \rightarrow 0, \bar{\theta} \rightarrow 0, \bar{\phi} \rightarrow 0 \end{aligned} \right\} \quad (25)$$

The system of differential equations (22), (23) and (24) are solved subject to (25), which are presented in Equations (26), (27) and (28).

$$\bar{q} = \left[\frac{1}{s} + \frac{Ra^2}{s^2} (1 - e^{-s}) \left(\frac{\lambda_6}{s - \lambda_7} + \frac{\lambda_8}{s - \lambda_9} \right) \right] e^{-y\sqrt{Ra(s+\lambda)}} - \frac{Ra^2}{s^2} (1 - e^{-s}) \left[\frac{\lambda_6}{s - \lambda_7} e^{-y\sqrt{\frac{s+\lambda_3}{\lambda_2}}} + \frac{\lambda_8}{s - \lambda_9} e^{-y\sqrt{\frac{s+\lambda_5}{\lambda_4}}} \right] \quad (26)$$

$$\bar{\theta} = \frac{1}{s^2} (1 - e^{-s}) e^{-y\sqrt{\frac{s+\lambda_3}{\lambda_2}}} \quad (27)$$

$$\bar{\phi} = \frac{1}{s^2} (1 - e^{-s}) e^{-y\sqrt{\frac{s+\lambda_5}{\lambda_4}}} \quad (28)$$

Now on imposition of inverse Laplace transformations on (26), (27) and (28), finally get the

expressions which describe the velocity distribution, temperature distribution and concentration profile of the problem defined in our study.

$$q = \left. \begin{aligned} & \psi_1 + \frac{\lambda_6 Ra^2}{\lambda_7^2} e^{\lambda_7(t-1)} (e^{\lambda_7} \psi_2 - \bar{\psi}_2) - \frac{\lambda_6 Ra^2}{\lambda_7} (f_1 - \bar{f}_1) - \frac{\lambda_6 Ra^2}{\lambda_7^2} (\psi_1 - \bar{\psi}_1) \\ & + \frac{\lambda_8 Ra^2}{\lambda_9^2} e^{\lambda_9(t-1)} (e^{\lambda_9} \psi_3 - \bar{\psi}_3) - \frac{\lambda_8 Ra^2}{\lambda_9} (f_1 - \bar{f}_1) - \frac{\lambda_8 Ra^2}{\lambda_9^2} (\psi_1 - \bar{\psi}_1) \\ & - \frac{\lambda_6 Ra^2}{\lambda_7^2} e^{\lambda_7(t-1)} (e^{\lambda_7} \psi_4 - \bar{\psi}_4) + \frac{\lambda_6 Ra^2}{\lambda_7} (f_2 - \bar{f}_2) + \frac{\lambda_6 Ra^2}{\lambda_7^2} (\psi_5 - \bar{\psi}_5) \\ & - \frac{\lambda_8 Ra^2}{\lambda_9^2} e^{\lambda_9(t-1)} (e^{\lambda_9} \psi_6 - \bar{\psi}_6) + \frac{\lambda_8 Ra^2}{\lambda_9} (f_3 - \bar{f}_3) + \frac{\lambda_8 Ra^2}{\lambda_9^2} (\psi_7 - \bar{\psi}_7) \end{aligned} \right\} \quad (29)$$

$$\theta = f_2 - \bar{f}_2 \quad (30)$$

$$\phi = f_3 - \bar{f}_3 \quad (31)$$

4. VELOCITY DISTRIBUTION FOR UNIT SCHMIDT NUMBER

It is to be noted that the velocity distribution given by (29) is not valid for $Sc=1$. As the Schmidt number is the ratio of the momentum diffusivity to mass diffusivity, unit Schmidt number refers to the case when velocity and concentration boundary layer thickness are of the same order in magnitude. We sometimes practically encounter fluid motions of this category. So, velocity distribution valid for $Sc=1$ is obtained by substituting $Sc=1$ in the governing equation (19) and then solving the differential equations proceeding with the same method applied earlier. Velocity distribution for unit Schmidt number is found to be,

$$q = \left. \begin{aligned} & \psi_1 + \frac{\lambda_6 Ra^2}{\lambda_7^2} e^{\lambda_7(t-1)} (e^{\lambda_7} \psi_2 - \bar{\psi}_2) - \frac{\lambda_6 Ra^2}{\lambda_7} (f_1 - \bar{f}_1) - \frac{\lambda_6 Ra^2}{\lambda_7^2} (\psi_1 - \bar{\psi}_1) \\ & + \lambda_{12} Ra^2 (f_1 - \bar{f}_1) - \frac{\lambda_6 Ra^2}{\lambda_7^2} e^{\lambda_7(t-1)} (e^{\lambda_7} \psi_4 - \bar{\psi}_4) + \frac{\lambda_6 Ra^2}{\lambda_7} (f_2 - \bar{f}_2) \\ & + \frac{\lambda_6 Ra^2}{\lambda_7^2} (\psi_5 - \bar{\psi}_5) - \lambda_{12} Ra^2 (f_4 - \bar{f}_4) \end{aligned} \right\} \quad (32)$$

It is noticed that concentration profile given by Equation (31) is valid for $Sc=1$ too and obviously there arises no question of validity on temperature distribution.

5. SKIN FRICTION

The coefficient of skin friction, C_f obtained to gauge the viscous drag at the plate arising due to the fluid motion is found to be as follows:

$$\begin{aligned}
 C_f &= -\left. \frac{\partial q}{\partial y} \right]_{y=0} \\
 &= \left. \begin{aligned}
 &\psi_1' + \frac{\lambda_6 Ra^2}{\lambda_7^2} e^{\lambda_7(t-1)} \left(e^{\lambda_7} \psi_2' - \bar{\psi}_2' \right) - \frac{\lambda_6 Ra^2}{\lambda_7} \left(f_1' - \bar{f}_1' \right) - \frac{\lambda_6 Ra^2}{\lambda_7^2} \left(\psi_1' - \bar{\psi}_1' \right) \\
 &+ \frac{\lambda_8 Ra^2}{\lambda_9^2} e^{\lambda_9(t-1)} \left(e^{\lambda_9} \psi_3' - \bar{\psi}_3' \right) - \frac{\lambda_8 Ra^2}{\lambda_9} \left(f_1' - \bar{f}_1' \right) - \frac{\lambda_8 Ra^2}{\lambda_9^2} \left(\psi_1' - \bar{\psi}_1' \right) \\
 &- \frac{\lambda_6 Ra^2}{\lambda_7^2} e^{\lambda_7(t-1)} \left(e^{\lambda_7} \psi_4' - \bar{\psi}_4' \right) + \frac{\lambda_6 Ra^2}{\lambda_7} \left(f_2' - \bar{f}_2' \right) + \frac{\lambda_6 Ra^2}{\lambda_7^2} \left(\psi_5' - \bar{\psi}_5' \right) \\
 &- \frac{\lambda_8 Ra^2}{\lambda_9^2} e^{\lambda_9(t-1)} \left(e^{\lambda_9} \psi_6' - \bar{\psi}_6' \right) + \frac{\lambda_8 Ra^2}{\lambda_9} \left(f_3' - \bar{f}_3' \right) + \frac{\lambda_8 Ra^2}{\lambda_9^2} \left(\psi_7' - \bar{\psi}_7' \right)
 \end{aligned} \right\} \quad (33)
 \end{aligned}$$

The corresponding C_f for $Sc=1$ is obtained as:

$$\begin{aligned}
 C_f \Big|_{Sc=1} &= \left. \begin{aligned}
 &\psi_1' + \frac{\lambda_6 Ra^2}{\lambda_7^2} e^{\lambda_7(t-1)} \left(e^{\lambda_7} \psi_2' - \bar{\psi}_2' \right) - \frac{\lambda_6 Ra^2}{\lambda_7} \left(f_1' - \bar{f}_1' \right) - \frac{\lambda_6 Ra^2}{\lambda_7^2} \left(\psi_1' - \bar{\psi}_1' \right) \\
 &+ \lambda_{12} Ra^2 \left(f_1' - \bar{f}_1' \right) - \frac{\lambda_6 Ra^2}{\lambda_7^2} e^{\lambda_7(t-1)} \left(e^{\lambda_7} \psi_4' - \bar{\psi}_4' \right) + \frac{\lambda_6 Ra^2}{\lambda_7} \left(f_2' - \bar{f}_2' \right) \\
 &+ \frac{\lambda_6 Ra^2}{\lambda_7^2} \left(\psi_5' - \bar{\psi}_5' \right) - \lambda_{12} Ra^2 \left(f_4' - \bar{f}_4' \right)
 \end{aligned} \right\} \quad (34)
 \end{aligned}$$

6. NUSSELT NUMBER AND SHERWOOD NUMBER

The rate of heat transfer from the plate in terms of Nusselt number and mass transfer rate at the plate in terms of Sherwood number are found as:

$$\text{Nu} = -\left. \frac{\partial \theta}{\partial y} \right]_{y=0} = f_2' - \bar{f}_2' \quad (35)$$

$$\text{Sh} = -\left. \frac{\partial \phi}{\partial y} \right]_{y=0} = f_3' - \bar{f}_3' \quad (36)$$

7. RESULTS AND DISCUSSION

Parameters that influence in our investigation at a particular time are Grashof number Gr , solutal Grashof number Gm , Ramped parameter Ra , Schmidt number Sc , magnetic parameter M , chemical reaction parameter K , permeability parameter Kp , sink of heat Q , Prandtl number Pr , Hall parameter β_e , rotational parameter Er and radiation parameter N . To analyze the outcomes of our investigation, these parameters are assigned admissible and realistic values and with the help of the Matlab software, velocity field (29), temperature distribution (30), concentration profile (31), skin friction (33), Nusselt number (35) and Sherwood number (36) are computed numerically and the results are presented graphically in the following.

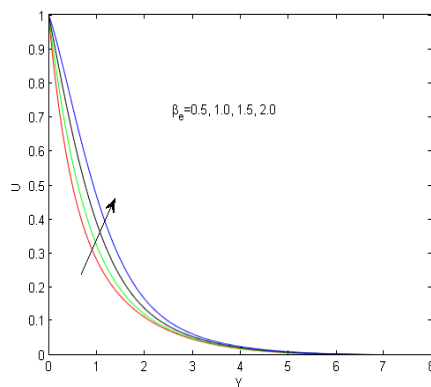


Fig 1: Primary velocity profile for $Gr=6; Gm=5; Kp=0.5; Ra=0.5;$
 $Pr=0.71; Kc=0.2; Sc=0.6; Er=0.02;$
 $M=5; t=1.2; Q=3; N=5$

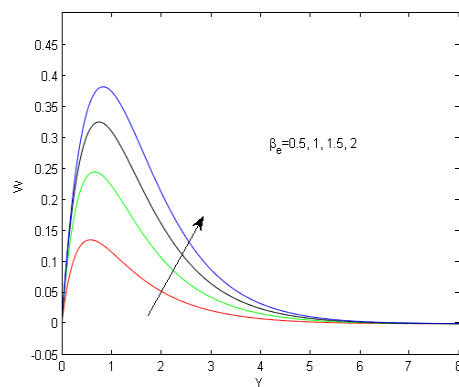


Fig 2: Secondary velocity profile for $Gr=6; Gm=5; Kp=0.5; Ra=0.5;$
 $Pr=0.71; Kc=0.2; Sc=0.6; Er=0.02;$
 $M=5; t=1.2; Q=3; N=5$

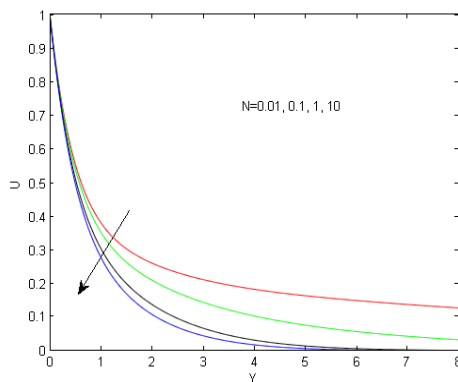


Fig 3: Primary velocity profile for $Gr=6; Gm=5; Kp=0.5; Ra=0.5;$
 $Pr=0.71; Kc=0.2; Sc=0.6; Er=0.02;$
 $M=5; t=1.2; Q=3; \beta_e=0.5$

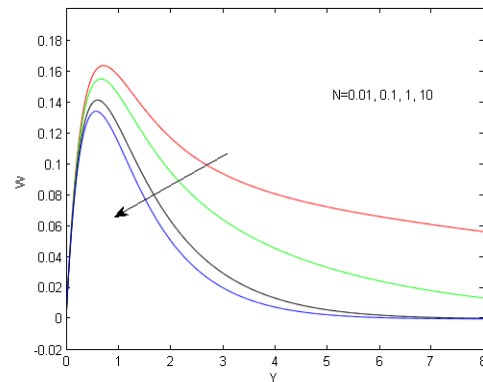


Fig 4: Secondary velocity profile for $Gr=6; Gm=5; Kp=0.5; Ra=0.5;$
 $Pr=0.71; Kc=0.2; Sc=0.6; Er=0.02;$
 $M=5; t=1.2; Q=3; \beta_e=0.5$

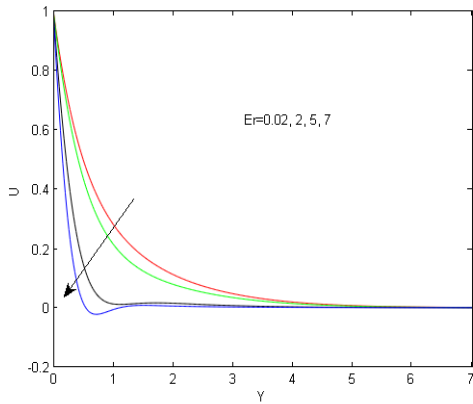


Fig 5: Primary velocity profile for $Gr=6; Gm=5; Kp=0.5; Ra=0.5; Pr=0.71; Kc=0.2; Sc=0.6; N=5; M=5; t=1.2; Q=3; \beta_e=0.5$

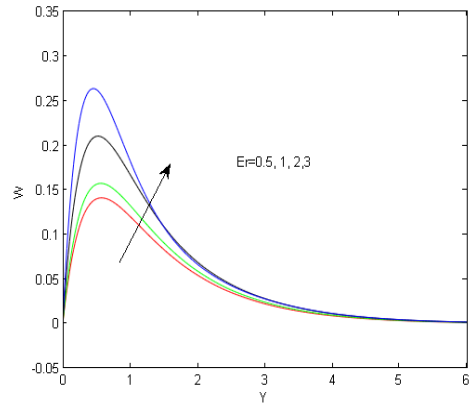


Fig 6: Secondary velocity profile for $Gr=6; Gm=5; Kp=0.5; Ra=0.5; Pr=0.71; Kc=0.2; Sc=0.6; N=5; M=5; t=1.2; Q=3; \beta_e=0.5$

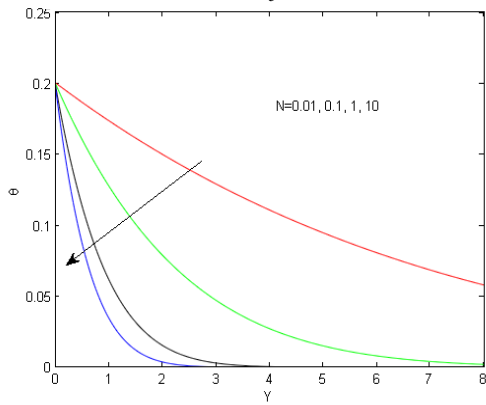


Fig 7: Temperature distribution for $Ra=0.5; Pr=0.71; t=0.2; Q=3$

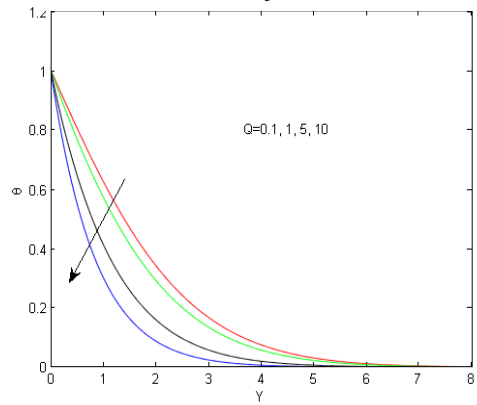


Fig 8: Temperature distribution for $Ra=0.5; Pr=0.71; t=0.2; N=5$

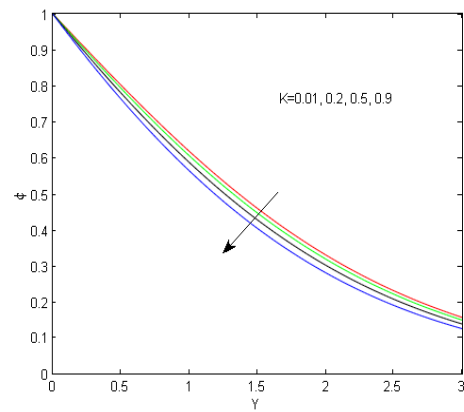


Fig 9: Concentration profile for $Ra=0.5; Sc=0.6; t=1.2$

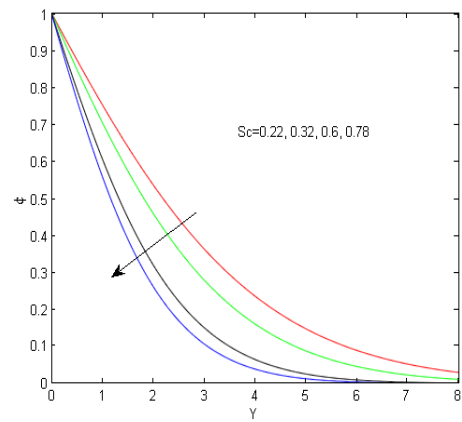


Fig 10: Concentration profile for $Ra=0.5; K=0.2; t=1.2$

ROTATING MHD CONVECTIVE HEAT AND MASS TRANSFER FLOW

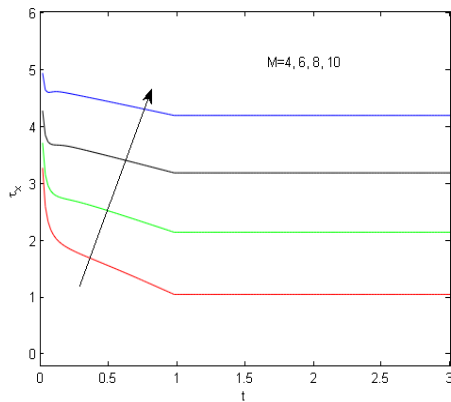


Fig 11: Primary skin friction for $Gr=6; Gm=5; Kp=0.5; Ra=0.5;$
 $Pr=0.71; Kc=0.2; Sc=0.6; Er=0.02;$
 $N=5; Q=3; \beta_e=0.5$

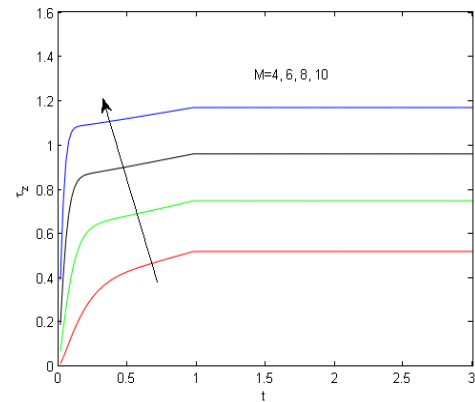


Fig 12: Secondary skin friction for $Gr=6; Gm=5; Kp=0.5; Ra=0.5;$
 $Pr=0.71; Kc=0.2; Sc=0.6; Er=0.02;$
 $N=5; Q=3; \beta_e=0.5$

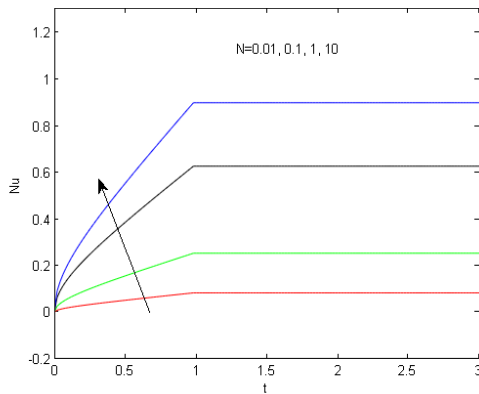


Fig 13: Nusselt number for $Ra=0.5;$
 $Pr=0.71; Q=3$

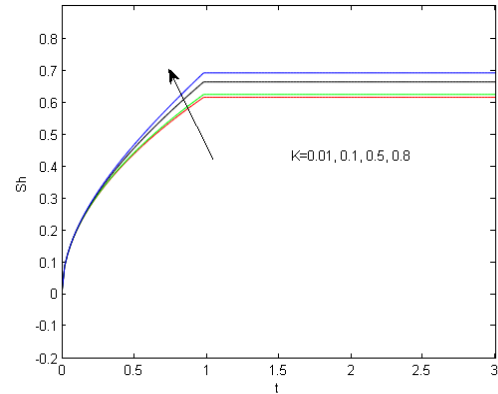


Fig 14: Sherwood number for $Ra=0.5;$
 $Sc=0.6$

The velocity is plotted against the normal coordinate Y . Primary velocity profile is presented in Figures 1, 3 and 5 and Figures 2, 4 and 6 represent the secondary velocity profile. Influence of the Hall current parameter on velocity is demonstrated in figures 1 and 2. Both the figures suggest that Hall current parameter catalyzes velocity in both directions. Effect of radiation parameter on the primary velocity is analyzed in Figure 3 and Figure 4 displays the radiation effect on the secondary velocity. As expected, as the system loses more energy in the form of radiation, velocity reduces. Coriolis force also has a significant impact on the velocity which is clear from Figures 5 and 6. Result of the increase in the rotational parameter is a negative growth of the primary velocity while it is a positive growth in the case of secondary velocity. Rotation slightly shifts the motion in the

secondary direction and so these findings are physically justified. One important characteristic established in all these six figures is that velocity goes on diminishing on moving further and further away from the plate. The exception is that secondary velocity first increases with distance up to certain point and then only starts diminishing. Primary velocity attains maximum magnitude near the plate because the force of buoyancy is experienced strongly in the neighborhood of the plate.

Figures 7 and 8 represent the temperature distribution of the system with respect to the normal coordinate in which influence of two important parameters radiation and heat sink are studied. Figure 7 illustrates that radiation lowers the temperature. Radiating fluid loses thermal energy and hence temperature in the process of radiation. A heat sink absorbs heat from the surrounding. So, the presence of a heat sink or heat absorber reduces the ambient fluid temperature which has been reflected in Figure 8. Fluid temperature at the plate is the highest and it decreases gradually away from the plate.

Figures 9 and 10 describe how fluid concentration is distributed. The two figures clearly indicate that like temperature, concentration too is highest at the plate and concentration level reduces with increasing distance from the plate. Figure 9 states that concentration can be lowered with a faster rate of chemical reaction. As mass diffusion increases the concentration of the diffusing medium and Schmidt number is inversely proportional to the mass diffusivity, increase in the Schmidt number lowers the concentration level as displayed in Figure 10.

The variation of skin friction at the plate with time both in the primary direction and secondary direction is presented in Figures 11 and 12 respectively. After initial variations, skin frictions become constant from time $t = 1$. Variations of the magnetic field parameters in both the figures establish that a strong magnetic field significantly increases the viscous drag. This is due to the Lorentz force acting in the opposite direction of the velocity.

The effect of radiation on the rate of rate of heat transfer and the effect of chemical reaction on the rate of mass transfer with respect to time are explained respectively by Figures 13 and 14. Heat transfer takes place through radiation also. So the increase of Nusselt number or acceleration of

the rate of heat transfer with radiation is observed in Figure 13. Figure 14 states that Sherwood number or rate of mass transfer at the plate enhances with faster rate of chemical reaction. This is the reason why we observe in Figure 9 the lowering of concentration level with chemical reaction. From time $t = 1$ onwards, both Nusselt and Sherwood number are constants.

8. CONCLUSIONS

The following conclusions are summarized based on our investigation:

- Hall current accelerates and radiation decelerates the velocity of both directions.
- Due to rotation, primary velocity decreases but secondary velocity increases.
- Presence of a heat sink decreases the fluid temperature.
- Increase in the Schmidt number lowers the concentration profile.
- Transversely applied magnetic field increases the drag force.
- Radiation accelerates the heat transfer and consequently drops the fluid temperature.
- Chemical reaction boosts the mass transfer rate and reduces the concentration.

NOMENCLATURE

a^* : Mean absorption coefficient

\vec{B} : Magnetic induction vector

B_0 : Magnitude of applied magnetic field

C' : Fluid concentration

C_f : Skin friction coefficient

C_p : Specific heat at constant pressure

D_M : Mass diffusivity

Er : Rotational parameter

\vec{g} : Acceleration due to gravity

G_m : Solutal Grashof number

Gr : Grashof number

\vec{J} : Current density vector

K : Chemical reaction parameter

K_1 : Chemical reaction constant

Kp : Permeability parameter

Kp^* : Permeability constant

M : Magnetic parameter

N : Radiation parameter

Nu : Nusselt number

p : Fluid pressure

Pr : Prandtl number

q_r : Radiative heat flux

Q : Sink of heat

Q' : First order heat sink

Ra : Ramped parameter

Sc : Schmidt number

Sh : Sherwood number

t' : Time

T' : Fluid temperature

β : Volume expansion coefficient for heat transfer

β^* : Volume expansion coefficient for mass transfer

β_e : Hall parameter

κ : Thermal conductivity

μ : Coefficient of viscosity

ν : Kinematic viscosity

ρ : Fluid density

σ : Electrical conductivity

σ^* : Stefan-Boltzman constant

ω : Angular speed

APPENDIX

$$\lambda = Ra \left\{ \frac{M^2}{1 + \beta_e^2} (1 - i\beta_e) + \frac{1}{Kp} - 2iEr^2 \right\} \quad \lambda_2 = \frac{1}{Pr Ra} \left(1 + \frac{4}{3N} \right) \quad \lambda_3 = QRa$$

$$\lambda_4 = \frac{1}{ScRa} \quad \lambda_5 = KRa \quad \lambda_6 = \frac{\lambda_2 Gr}{1 - Ra\lambda_2} \quad \lambda_7 = \frac{Ra\lambda\lambda_2 - \lambda_3}{1 - Ra\lambda_2}$$

$$\lambda_8 = \frac{\lambda_4 Gm}{1 - Ra\lambda_4} \quad \lambda_9 = \frac{Ra\lambda\lambda_4 - \lambda_5}{1 - Ra\lambda_4} \quad \lambda_{10} = \frac{1}{\lambda_4} \quad \lambda_{11} = \frac{1}{\lambda_2} \quad \lambda_{12} = \frac{Gm}{Ra(\lambda_5 - \lambda)}$$

$$\psi(\xi, \eta, y, t) = \frac{1}{2} \left[e^{\sqrt{\xi\eta}y} \operatorname{erfc} \left(\frac{\sqrt{\xi}y}{2\sqrt{t}} + \sqrt{\eta t} \right) + e^{-\sqrt{\xi\eta}y} \operatorname{erfc} \left(\frac{\sqrt{\xi}y}{2\sqrt{t}} - \sqrt{\eta t} \right) \right]$$

$$\bar{\psi}(\xi, \eta, y, t) = \psi(\xi, \eta, y, t-1)H(t-1)$$

$$\psi'(\xi, \eta, t) = \sqrt{\xi\eta} \operatorname{erf}(\sqrt{\eta t}) + e^{-\eta t} \sqrt{\frac{\xi}{\pi t}}$$

$$\bar{\psi}'(\xi, \eta, t) = \psi'(\xi, \eta, t-1)H(t-1)$$

$$f(\xi, \eta, y, t) = \left(\frac{t}{2} + \frac{y\sqrt{\xi}}{4\sqrt{\eta}} \right) e^{\sqrt{\xi\eta}y} \operatorname{erfc} \left(\frac{\sqrt{\xi}y}{2\sqrt{t}} + \sqrt{\eta t} \right) + \left(\frac{t}{2} - \frac{y\sqrt{\xi}}{4\sqrt{\eta}} \right) e^{-\sqrt{\xi\eta}y} \operatorname{erfc} \left(\frac{\sqrt{\xi}y}{2\sqrt{t}} - \sqrt{\eta t} \right)$$

$$\bar{f}(\xi, \eta, y, t) = f(\xi, \eta, y, t-1)H(t-1)$$

$$f'(\xi, \eta, t) = t\sqrt{\xi\eta} \operatorname{erf}(\sqrt{\eta t}) + e^{-\eta t} \sqrt{\frac{\xi t}{\pi}} + \frac{\sqrt{\xi}}{2\sqrt{\eta}} \operatorname{erf}(\sqrt{\eta t})$$

$$\bar{f}'(\xi, \eta, t) = f'(\xi, \eta, t-1)H(t-1)$$

$$\psi_1 = \psi(Ra, \lambda, y, t)$$

$$\psi_2 = \psi(Ra, \lambda_7 + \lambda, y, t)$$

$$\psi_3 = \psi(Ra, \lambda_9 + \lambda, y, t)$$

$$\psi_4 = \psi(\lambda_{11}, \lambda_7 + \lambda_3, y, t)$$

$$\psi_5 = \psi(\lambda_{11}, \lambda_3, y, t)$$

$$\psi_6 = \psi(\lambda_{10}, \lambda_9 + \lambda_5, y, t)$$

$$\psi_7 = \psi(\lambda_{10}, \lambda_5, y, t)$$

$$\bar{\psi}_1 = \bar{\psi}(Ra, \lambda, y, t)$$

$$\bar{\psi}_2 = \bar{\psi}(Ra, \lambda_7 + \lambda, y, t)$$

$$\bar{\psi}_3 = \bar{\psi}(Ra, \lambda_9 + \lambda, y, t)$$

$$\bar{\psi}_4 = \bar{\psi}(\lambda_{11}, \lambda_7 + \lambda_3, y, t)$$

$$\bar{\psi}_5 = \bar{\psi}(\lambda_{11}, \lambda_3, y, t)$$

$$\bar{\psi}_6 = \bar{\psi}(\lambda_{10}, \lambda_9 + \lambda_5, y, t)$$

$$\bar{\psi}_7 = \bar{\psi}(\lambda_{10}, \lambda_5, y, t)$$

$$\psi'_1 = \psi'(Ra, \lambda, t)$$

$$\psi'_2 = \psi'(Ra, \lambda_7 + \lambda, t)$$

$$\psi'_3 = \psi'(Ra, \lambda_9 + \lambda, t)$$

$$\psi'_4 = \psi'(\lambda_{11}, \lambda_7 + \lambda_3, t)$$

$$\psi'_5 = \psi'(\lambda_{11}, \lambda_3, t)$$

$$\psi'_6 = \psi'(\lambda_{10}, \lambda_9 + \lambda_5, t)$$

$$\psi'_7 = \psi'(\lambda_{10}, \lambda_5, t)$$

$$\bar{\psi}'_1 = \bar{\psi}'(Ra, \lambda, t)$$

$$\bar{\psi}'_2 = \bar{\psi}'(Ra, \lambda_7 + \lambda, t)$$

$$\bar{\psi}'_3 = \bar{\psi}'(Ra, \lambda_9 + \lambda, t)$$

$$\bar{\psi}'_4 = \bar{\psi}'(\lambda_{11}, \lambda_7 + \lambda_3, t)$$

$$\bar{\psi}'_5 = \bar{\psi}'(\lambda_{11}, \lambda_3, t)$$

$$\bar{\psi}'_6 = \bar{\psi}'(\lambda_{10}, \lambda_9 + \lambda_5, t)$$

$$\bar{\psi}'_7 = \bar{\psi}'(\lambda_{10}, \lambda_5, t)$$

$$f_1 = f(Ra, \lambda, y, t)$$

$$f_2 = f(\lambda_{11}, \lambda_3, y, t)$$

$$f_3 = f(\lambda_{10}, \lambda_5, y, t)$$

$$f_4 = f(Ra, \lambda_5, y, t)$$

$$\bar{f}_1 = \bar{f}(Ra, \lambda, y, t)$$

$$\bar{f}_2 = \bar{f}(\lambda_{11}, \lambda_3, y, t)$$

$$\bar{f}_3 = \bar{f}(\lambda_{10}, \lambda_5, y, t)$$

$$\bar{f}_4 = \bar{f}(Ra, \lambda_5, y, t)$$

$$f'_1 = f'(Ra, \lambda, t)$$

$$f'_2 = f'(\lambda_{11}, \lambda_3, t)$$

$$f'_3 = f'(\lambda_{10}, \lambda_5, t)$$

$$f_4' = f'(Ra, \lambda_5, t)$$

$$\bar{f}_1' = \bar{f}'(Ra, \lambda, t)$$

$$\bar{f}_2' = \bar{f}'(\lambda_{11}, \lambda_3, t)$$

$$\bar{f}_3' = \bar{f}'(\lambda_{10}, \lambda_5, t)$$

$$\bar{f}_4' = \bar{f}'(Ra, \lambda_5, t)$$

CONFLICT OF INTERESTS

The author(s) declare that there is no conflict of interests.

REFERENCES

- [1] T. G. Cowling, *Magneto hydrodynamics*, Wiley Inter Science, New York, (1957).
- [2] I. Pop, The effect of Hall currents on hydromagnetic flow near an accelerated plate, *J. Math. Phys Sci.* 5(1971), 375.
- [3] K. R. Cramer, S. I. Pai, *Magnetofluid Dynamics for Engineers and Applied Physicists*, McGraw-Hill, New York, USA, (1973).
- [4] H. S. Takhar, S. Roy, G. Nath, Unsteady free convection flow over an infinite vertical porous plate due to the combined effects of thermal and mass diffusion, magnetic field and Hall currents, *Heat Mass Transfer.* 39 (2003), 825-834.
- [5] M. A. Maleque, M. A. Sattar, The effects of variable properties and Hall current on steady MHD laminar convective fluid flow due to a porous rotating disk, *Int. J. Heat Mass Transfer*, 48 (23-24) (2005), 4963-4972.
- [6] N. Ahmed, H. K. Sarmah, MHD transient flow past an impulsively started infinite horizontal porous plate in a rotating system with Hall current, *Int. J. Appl. Math. Mech.* 7 (2) (2011), 1-15.
- [7] S. K. Ghosh, O. A. Beg, S. Rawat, T. A. Beg, Three dimensional rotating hydromagnetic transient convection flow of liquid metal in a porous medium with Hall and ionslip current effects, *Emirates J. Eng. Res.* 14(2) (2009), 45-57.

- [8] G. S. Seth, G. K. Mahato, S. Sarkar, Effects of Hall current and rotation on MHD natural convection flow past an impulsively moving vertical plate with ramped temperature in the presence of thermal diffusion with heat absorption, *Int. J. Energy Technol.* 5(16) (2013), 1-12.
- [9] G. S. Seth, S. Sarkar, S. M. Hussain, G. K. Mahato, Effects of Hall current and rotation on hydromagnetic natural convection flow with heat and mass transfer of a heat absorbing fluid past an impulsively moving vertical plate with ramped temperature, *J. Appl. Fluid Mech.* 8(1) (2015), 159-171.
- [10] M. M. Ali, T. S. Chen, B. F. Armaly, Natural convection-radiation interaction in boundary-layer flow over horizontal surfaces, *AIAA J.* 22(12) (1984), 1797-1803.
- [11] M. A. Mansour, Radiation and free convection effects on the oscillating flow past a vertical plate, *Astrophys. Space Sci.* 166(2) (1990), 269-275.
- [12] O. D. Makinde, Free convection flow with thermal radiation and mass transfer past a moving vertical porous plate, *Int. Commun. Heat Mass Transfer.* 32 (2005), 1411-1419.
- [13] I. U. Mbeledogu, A. R. C. Amakiri and A. Ogulu, Unsteady MHD free convection flow of a compressible fluid past a moving vertical plate in the presence of radiative heat transfer, *Int. J. Heat Mass Transfer.* 50(9-10) (2007), 326-331.
- [14] N. Ahmed, Soret and radiation effects on transient MHD free convection from an impulsively started infinite vertical plate. *J. Heat Transf.* 134 (2012), 062701.
- [15] N. Ahmed, Buoyancy induced MHD transient mass transfer flow with thermal radiation, *Alexandria Eng. J.* 55(3) (2016), 2321-2331.
- [16] K. Choudhury, N. Ahmed, Unsteady MHD mass transfer flow past a temporarily accelerated semi-infinite vertical plate in presence of thermal diffusion with ramped wall temperature, *Math. Model. Eng. Probl.* 6(2) (2019), 241-248.
- [17] S. Jena, G. C. Dash, S. R. Mishra, Chemical reaction effect on MHD viscoelastic fluid flow over a vertical stretching sheet with heat source/sink, *Ain Shams Eng. J.* 9(4) (2018), 1205-1213.
- [18] D. Gurram, K. S. Balamurugan, V. C. C. Raju, N. Vedavathi, Effect of chemical reaction on MHD Casson fluid flow past an inclined surface with radiation, *Skit Res. J.* 7(1) (2017), 53-59.